ReprintsDesk | 3/10/2026 9:56:08 PM

Antibody Targeting in Metastatic Colon Cancer: A Phase I Study of Monoclonal Antibody F19 Against a Cell-Surface Protein of Reactive Tumor Stromal Fibroblasts

By Sydney Welt, Chaitanya R. Divgi, Andrew M. Scott, Pilar Garin-Chesa, Ronald D. Finn, Martin Graham, Elizabeth A. Carswell, Alfred Cohen, Steven M. Larson, Lloyd J. Old, and Wolfgang J. Rettig

Purpose: **To define the toxicity, imaging, and biodistribution characteristics of iodine 131-labeled monoclonal antibody F19 (^{131}I-mAbF19). MAbF19 recognizes the fibroblast activation protein (FAP), a cell-surface glycoprotein not present in most normal tissues, but abundantly expressed by reactive stromal fibroblasts of epithelial cancers, including more than 95% of primary and metastatic colorectal carcinomas.**

Patients and Methods: **^{131}I-mAbF19 was administered intravenously to 17 patients with hepatic metastases from colorectal carcinoma who were scheduled for resection of localized metastases or insertion of hepatic artery catheter for regional chemotherapy. Seven to 8 days before surgery, patients received ^{131}I-mAbF19 at three dose levels, with at least four patients entered at each level.**

Results: **No toxicity associated with intravenous ^{131}I-mAbF19 administration was observed. Tumor images were obtained on planar and single-photon emission tomography (SPECT) scans in 15 of 17 patients with hepatic metastases, tumor-infiltrated portal lymph nodes, and/or recurrent pelvic disease. The smallest lesion visualized was 1 cm in diameter. The optimal time for tumor imaging was 3 to 5 days after ^{131}I-mAbF19 administration. The use of image registration techniques allowed precise anatomic localization of ^{131}I-mAbF19 accumulation. Immunohistochemical analysis of biopsy tissues showed expression of FAP in the tumor stroma (but not in normal liver) in all patients studied and confirmed that the FAP-positive tumor stromal fibroblasts were interposed between the tumor capillaries and the malignant colon epithelial cells. At the time of surgery, tumor-to-liver ratios up to 21:1 and tumor-to-serum ratios up to 9:1 were obtained. The fraction of the injected ^{131}I-mAbF19 dose per gram tumor (%ID/g tumor) localized to hepatic metastases at the time of surgery ranged from 0.001% to 0.016%.**

Conclusion: **The FAP tumor fibroblast antigen is highly expressed in primary and metastatic colorectal carcinomas and shows limited expression in normal adult tissues. This highly selective expression pattern allows imaging of colorectal carcinoma lesions as small as 1 cm in diameter on ^{131}I-mAbF19 scans. Because of the consistent presence of FAP in the stroma of epithelial cancers and the accessibility of FAP-positive tumor stromal fibroblasts to circulating monoclonal antibodies (mAbs), this study suggests possible diagnostic and therapeutic applications of humanized mAbF19 and mAbF19 constructs with novel immune and nonimmune effector functions.**

J Clin Oncol 12:1193-1203. ***© 1994 by American Society of Clinical Oncology.***

THE USE OF monoclonal antibodies (mAbs) as targeting agents for cancer detection and therapy continues to attract much attention despite the many technical challenges that confront its successful clinical application.[1-10] Major limitations in the systemic use of mAbs in cancer patients encountered in previous studies include the following: (1) shared antigen expression on normal and neoplastic cells; (2) variability in antigen expression in histologically similar tumors in different patients or among distinct lesions in the same patient (antigenic heterogeneity); (3) low accessibility of tumor antigens to mAbs circulating in the blood stream; (4) immunoselection of antigen-loss variants during mAb therapy; and (5) immunogenicity of the murine mAbs used in clinical studies.

However, in the past few years, each of these obstacles has become amenable to new approaches, using improved techniques and reagents for target identification,[11] the construction of humanized and reshaped mAbs with low immunogenicity,[12] and the design of mAb conjugates or recombinant immunoglobulin (Ig) constructs with improved pharmacokinetic properties and/or enhanced immune or nonimmune effector functions.[13-19]

The initial search for antigenic targets in epithelial cancers has focused on cell-surface molecules of the transformed epithelium; as a result, a large number of epithelial membrane antigens have been identified and characterized with immunochemical and molecular genetic methods. However, only a handful of these antigens have shown the requisite tissue specificity to justify clinical evaluation in patients.[1-4,20,21] Therefore, an important challenge for most of the common types of epithelial cancers,

From the Ludwig Institute for Cancer Research, New York Unit; and Memorial Sloan-Kettering Cancer Center, New York, NY.

Submitted December 16, 1993; accepted February 11, 1994.

Supported in part by the Ludwig Institute for Cancer Research, grants from the National Cancer Institute, Bethesda, MD (CA-08748, CA-57486, and CA-33049), and the Oliver S. and Jennie R. Donaldson Charitable Trust, Inc.

Address reprint requests to Sydney Welt, MD, Ludwig Institute for Cancer Research, Memorial Sloan-Kettering Cancer Center, 1275 York Ave, New York, NY 10021.

© 1994 by American Society of Clinical Oncology.

0732-183X/94/1206-0015$3.00/0

Johns Hopkins University EX2033
GE Healthcare v. Johns Hopkins
IPR2026-00069

ReprintsDesk | 3/10/2026 9:56:08 PM

including colorectal carcinomas, remains the identification of additional antigenic targets for in vivo evaluation.

Surface antigens of transformed epithelial cells are still the most commonly studied antigenic targets in carcinomas, but the search for alternative targets in the cancer stroma has attracted much recent attention.[22-28] The stromal compartment of epithelial cancers consists of newly formed blood vessels, reactive fibroblasts, extracellular matrix proteins, and variable lymphoid and phagocytic infiltrates. The stromal compartment commonly makes up 20% to 50% of the mass of epithelial cancers, but in lesions with desmoplastic reactions may comprise up to 90% of the tumor mass. Studies with animal and human tumors suggest that stroma formation, including the formation of new tumor blood vessels, is critical for allowing solid tumors to grow beyond a size of approximately 1 to 2 mm in diameter. Tumor stromal cells, although not transformed, show a distinct functional program and may express inducible activation antigens not found on the corresponding resting cells in normal tissues. Endothelial and fibroblast activation antigens provide attractive targets for cancer detection and therapy, because they are highly accessible to circulating mAb, are shared by different histologic types of carcinomas (thus allowing the design of common therapies), and are expressed more uniformly and more stably than antigens of malignant cells, which are notorious for their genetic and phenotypic instability.

An extensively studied example of an inducible tumor stromal antigen of epithelial cancers is the fibroblast activation protein (FAP) defined by mAbF19 and additional mAbs against different FAP epitopes. FAP is a 95-kd cell-surface glycoprotein, and the gene encoding FAP has recently been isolated and characterized[29,30] (Rettig WJ: unpublished results). Immunohistochemical studies have shown that FAP is abundantly expressed in reactive stromal fibroblasts of more than 90% of common epithelial cancers, including colorectal carcinomas.[27,30,31] By contrast, FAP shows a limited distribution pattern in normal tissues. In an extensive survey of normal fetal and adult human tissues, FAP was detected only in a subset of endocrine cells (A cells) in the pancreas, and transiently in some fetal mesenchymal cells; FAP is also transiently expressed in the granulation tissue of healing wounds.[27,30,31] While FAP is consistently expressed in the stroma of malignant epithelial cancers, the stroma of benign epithelial tumors derived from the same organs is generally FAP-negative, suggesting that FAP may be induced by factors specifically released from malignant epithelial cells.

The present study was designed to determine the toxicity, pharmacokinetics, and biodistribution of iodine 131-labeled mAbF19 (^{131}I-mAbF19; anti-FAP) in patients with hepatic metastases from colorectal carcinoma and to evaluate the feasibility of localizing mAbs to the stromal compartment of solid tumors.

PATIENTS AND METHODS

Patient Characteristics

Seventeen patients with a histologically proven diagnosis of colorectal carcinoma were studied: 10 men aged 51 to 65 years (mean, 58.6) and seven women aged 47 to 74 years (mean, 63); patient characteristics are listed in Table 1. All patients were scheduled for one of the following surgical procedures: resection of localized liver metastases, insertion of hepatic artery catheter for regional chemotherapy of unresectable liver metastases, or resection of isolated extrahepatic metastases. The Karnofsky performance status of all patients was greater than 70%. None of the patients had received immunotherapy, chemotherapy, or radiation therapy within the preceding 4 weeks. Eligibility criteria included serum creatinine levels less than 2 mg/mL, granulocyte counts greater than 1,500/μL, platelet counts greater than 100,000/μL, and prothrombin time less than 1.3 $\times$ control. Patients with serious cardiac disease (New York State Heart Association Class III to IV), pulmonary disease, infectious disease requiring antibiotic therapy, prior exposure to mouse Ig, pregnancy or lactation, or an expected survival less than 6 weeks were excluded. Chest x-rays and computed tomographic (CT) scans (with intravenous contrast) of the chest and abdomen were obtained in all patients within 1 month before antibody infusion. In addition, magnetic resonance imaging (MRI) scans were obtained for some patients, and arteriograms of the celiac axis were performed in patients considered for hepatic artery catheter pump placement.

Informed consent was obtained from all patients before participation in the study; the study and consent forms were approved by the Institutional Review Board (IRB) of Memorial Sloan-Kettering Cancer Center (IRB no. 90-72).

Production and Purification of mAbF19

The generation, characterization, and reactivity of mAbF19 have been described previously.[27,29-31] To produce mAbF19 for clinical studies, F19 hybridoma cells were grown as ascites in pristane-treated (0.2 mL intraperitoneally), irradiated (3 Gy) CByB6F$_1$/J mice (Jackson Laboratories, Bar Harbor, ME). Ascites with high antibody titers were pooled and ultracentrifuged at 135,000 $\times g$ to remove cell debris and lipoproteins. The IgG fraction was precipitated with 40% ammonium sulfate, redissolved in 150 mmol/L sodium chloride (NaCl)/50 mmol/L tris, pH 8.9, passed over a Sephadex G25M column equilibrated in the same buffer, and chromatographed over protein A-Sepharose CL4B (Pharmacia LKB, Piscataway, NJ). The antibody was eluted with 50 mmol/L citrate/150 mmol/L NaCl, pH 5.0. After changing the buffer to 25 mmol/L phosphate/25 mmol/L NaCl, pH 6.0, on a Sephadex G25M column, the Ig fraction was further purified by high-performance cation-exchange chromatography (FPLC; Pharmacia) on a Mono S HR16/10 column. All procedures were performed aseptically with pyrogen-free material and, after each chromatographic step, the antibody was passed through a 0.2-μm Millex-GV filter (Millipore, Bedford, MA). Purity was evaluated by sodium dodecyl sulfate polyacrylamide gel electrophoresis followed by silver staining. The lot of purified mAbF19 used for clinical tests met standards set by the Food and Drug Administration, including tests for murine viruses, rabbit pyrogenicity, endotoxin

ReprintsDesk | 3/10/2026 9:56:08 PM

Table 1. Patient Characteristics

Patient No.	^{131}I-mAbF19 Dose (mg/m^2)	Age (years)/Sex	CEA* (ng/mL)	Biopsy (^{131}I count)	FAP Immunohistochemistry† Tumor Epithelial Cells	FAP Immunohistochemistry† Tumor Stroma	FAP Immunohistochemistry† Liver
1	0.2	64/M	91	Yes	−	++	−
2	0.2	59/F	1,800	Yes	−	++	−
3	0.2	66/F	158	NA	−	++	−
4	0.2	55/M	14	Yes	−	+++	−
5	0.2	55/M	79	Yes	−	+++	−
6	0.2	58/M	3,750	Yes	−	++	−
7	0.2	65/M	21	Yes	−	++	−
8	2	68/F	350	Yes	−	++	−
9	2	74/F	193	Yes		NA	
10	2	47/F	181	Yes	−	+	−
11	2	62/M	157	NA	−	+++	−
12	8	56/M	26	NA		NA	
13	8	66/F	256	Yes	−	+++	−‡
14	8	61/F	20	NA		NA	
15	8	64/M	23	Yes	−	++	−
16	8	51/M	15	Yes	−	+++	−
17	8	56/M	39	Yes	−	+++	−

Abbreviations: M, male; F, female; CEA, carcinoembryonic antigen; NA, sufficient biopsy material not available for radioactivity counting and/or immunohistochemistry.

*CEA normal range, 0 to 5.0 ng/mL.

†Results of immunohistochemical assays with mAbF19 are indicated as follows: +++, ++, +, abundant, intermediate, or scanty tumor stroma containing FAP-positive fibroblasts, respectively (compare with Fig 8); −, FAP-negative.

‡Normal colon mucosa of patient no. 13 tested (no normal liver biopsy available).

(limulus assays), bacterial and mycoplasma contamination, DNA content (< 10 pg at the highest administered dose), and mouse and guinea pig safety.

Radioiodination of mAbF19

Purified mAbF19 was labeled with 10 mCi of ^{131}I (New England Nuclear, Boston, MA) using the chloramine T method. The reaction was quenched with sodium metabisulfide, and the product was passed over a Sephadex G25 column (Pharmacia) prewashed with sterile 0.15 mol/L NaCl/5% human serum albumin (HSA). Fractions with peak activity were pooled and passed through a 0.22-μm Millex-GV filter. Freshly prepared clinical samples were tested for ^{131}I-binding to mAbF19 by trichloroacetic acid (TCA) precipitation to confirm radiolabeling efficiency. Immunoreactivity was assessed by sequential absorptions of ^{131}I-mAbF19 to pellets of FAP-positive SW872 sarcoma cells.[20] The final ^{131}I-mAbF19 preparations showed 33.2% ± 9.2% (0.2-mg dose level), 34.5% ± 9.9% (2-mg dose level), and 67.8% ± 9.3% immunoreactivity (8-mg dose level), respectively, and greater than 95% of the ^{131}I was TCA-precipitable.

Administration of Radiolabeled Antibody

Patients received 10 drops of a saturated solution of potassium iodide orally three times a day, beginning on the day of mAb administration and continuing to the time of surgery. ^{131}I-mAbF19 was administered intravenously in 0.9% NaCl with 5% HSA (total volume, 100 mL) through a 0.22-μm Millex-GV filter (Millipore, Bedford, MA) over 1 hour. Seven patients were entered at the 0.2-mg dose level, four patients at the 2-mg dose level, and six patients at the 8-mg dose level (Table 1).

Planar and Single-Photon Emission Computed Tomography Imaging

Anterior and posterior whole-body images were obtained 1 to 4 hours after antibody infusion, after 3 to 4 days, and on the day before surgery (day 6 or 7). Images were acquired with a Gemini 700 gamma camera (Technicare, Cleveland, OH) equipped with a high-energy collimator and linked to an ADAC 3300 computer (Milpitas, CA). Single-photon emission CT (SPECT) images were obtained 3 to 4 days after antibody infusion (64 stops, 30 to 40 seconds per stop, in a 64 × 64 × 8 matrix). Reconstruction of SPECT images was performed on a Pegasys workstation (ADAC) with a Butterworth filter (cutoff 0.3 to 0.4, order 5 to 15) and Chang attenuation correction.

SPECT and CT Image Registration

Image registration of SPECT and CT scans for precise anatomic localization of ^{131}I-mAbF19 uptake was also performed, using a previously described technique.[32,33] Briefly, CT images were digitized from original films by image capture with a video camera into an IBM-compatible personal computer. CT (or MRI) and SPECT image data sets were then transferred to a DEC Micro VAX II computer (Maynard, CA), and three-dimensional surface contours of the CT (or MRI) and SPECT images were outlined using contours on serial axial slices around internal landmarks (usually the liver). The three-dimensional surface outlines of the SPECT and CT images were fitted using an algorithm described by Pelizzari et al.[34] Corresponding axial SPECT and CT (or MRI) slices were displayed both separately and merged together (colorwash display) to allow anatomic localization of antibody uptake.

ReprintsDesk | 3/10/2026 9:56:08 PM

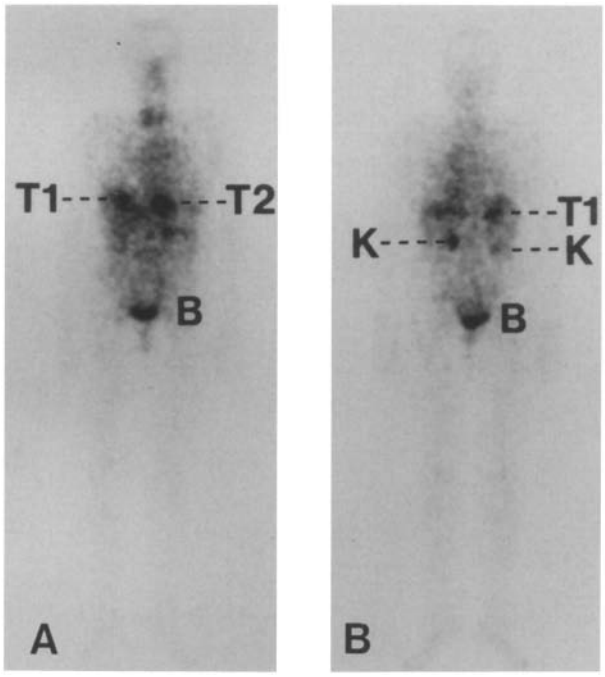

Fig 1. (A) Anterior and (B) posterior planar images of patient no. 3 obtained 4 days postinfusion of ^{131}I-mAbF19. Uptake of ^{131}I-mAbF19 is seen in 2 metastatic lesions in the liver (T1 and T2). Minimal blood-pool activity is seen in the chest. Accumulation of ^{131}I is also identified in the renal pelvis (K) and bladder (B) due to excretion of free iodine.

Biopsies and Blood Samples

Blood was drawn at 5, 15, 30, and 45 minutes and at 1, 2, 4 hours after ^{131}I-mAbF19 administration, before each image, and at the time of surgery. Decay-corrected data were used for calculating ^{131}I-mAbF19 blood clearance and uptake in tumor and liver biopsies, with results expressed as percent of injected dose (%ID) per liter or %ID per gram of tissue. Tissue biopsy samples were processed in the Department of Pathology, Memorial Hospital, for routine histopathologic evaluation; portions of the tissue samples were used for calculating the uptake of ^{131}I-mAbF19 based on radioactivity and for immunohistochemical investigations.

Blood activity data were analyzed with a graphical analysis program (BLD; Department of Nuclear Medicine, National Institutes of Health, Bethesda MD). Exponential curve fitting was performed to calculate the half-life ($T_{1/2}$) alpha and $T_{1/2}$ beta of the plasma clearance and the volume of distribution for ^{131}I-mAbF19.

Immunohistochemistry

The avidin-biotin immunoperoxidase method for antigen detection in tissue biopsy samples was performed as previously described.[27,30,31] Briefly, tissues were embedded in Tissue-Tek O.C.T. compound (Miles, Elkhart, IN), snap-frozen in isopentane precooled in liquid nitrogen, and stored at −70°C. Sections of 5 μm were cut, mounted on gelatin-coated slides, air-dried, and fixed in cold acetone for 10 minutes before immunoperoxidase staining with the Vectastain kit (Vector Laboratories, Burlingame, CA) according to the manufacturer's recommendations. The antibodies used were mAbF19,[29] mAbH572 (specific for endoGlyx-1, an endothelial-specific cell-surface antigen; Sanz-Moncasi MP: unpublished results), mAbA33[20] (specific for a cell-surface antigen of normal and malignant colonic epithelial cells), mAbNEC1a/b[35] (specific for the extracellular matrix protein tenascin), and negative control mouse IgG1 at 5 to 10 μg/mL. Sections were counterstained with Harris' hematoxylin.

Determination of Human Antimouse Ig Antibodies

Microwell plates (Nunc, Roskilde, Denmark) were incubated overnight with 10 μL of 100 μg/mL mAbF19 IgG or irrelevant mouse mAb IgG1. After blocking with 1% bovine serum albumin/phosphate-buffered saline, serial dilutions of patient sera were added, incubated for 2 hours, washed, incubated with class-specific antihuman Ig reagents (ICN Biomedicals, Lisle, IL), and developed by the alkaline phosphatase method.

RESULTS

Table 1 lists the characteristics of the 17 patients entered onto this trial. No toxicity related to antibody administration was observed during the course of this study. Serologic analysis of multiple blood samples obtained from the patients showed human anti-mouse Ig antibody responses of IgG and IgM subclass in all cases, with titers ranging from 10^{-2} to 10^{-4} 2 to 6 weeks after ^{131}I-mAbF19 administration.

Planar and SPECT Imaging Studies With ^{131}I-mAbF19

Sequential imaging studies in all patients showed gradual clearance of liver and spleen activity with time, consistent with blood-pool activity clearance (Figs 1 and 2). SPECT imaging was more sensitive than planar imaging, detecting lesions down to 1 cm in diameter. The optimal time for imaging was found to be 3 to 5 days after ^{131}I-

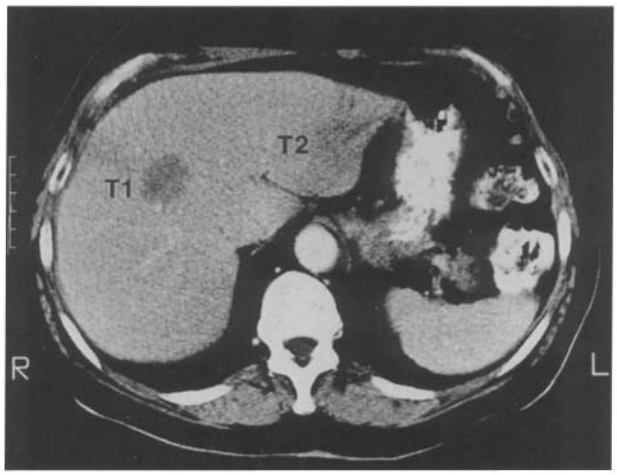

Fig 2. CT scan section of the liver of patient no. 3, shown in Fig 1. The 2 metastatic lesions can be identified in the right and left lobes of the liver, respectively, and correspond precisely to the areas of uptake in the planar ^{131}I-mAbF19 images.

ReprintsDesk | 3/10/2026 9:56:08 PM

mAbF19 injection, with some decrease in tumor to background contrast by day 7 (day of surgery).

Comparison of preoperative CT/MRI scans and SPECT studies to operative findings was performed (Table 2). Selective tumor localization of ^{131}I-mAbF19 was identified on planar and SPECT images in 15 of 16 patients with hepatic metastases ≥ 2 cm in diameter found at surgery. In one patient (no. 16), who had a negative planar imaging study, CT scans were positive preoperatively. Two patients (no. 5 and 10) had hepatic lesions 2 to 3 cm in diameter that were identified with SPECT but were negative on CT scans. Two additional patients with equivocal CT/MRI scans at the site of original colon surgery were found at the present surgery to have recurrent disease, and ^{131}I-mAbF19 SPECT studies were positive in one of these patients (no. 5). Pathologically confirmed portal lymph node disease was detected in only two of four patients with CT, and one of four patients with SPECT. CT detected 1-cm lung lesions not seen on SPECT, and both CT and SPECT failed to detect visceral seeding in one patient.

CT/SPECT Image Registration

Image registration considerably improved the ability to anatomically localize sites of ^{131}I-mAbF19 SPECT uptake (Figs 3 to 5). An example of this is patient no. 5, who had a history of an increasing carcinoembryonic antigen (CEA) serum level, a solitary right lobe liver lesion, and equivocal CT changes at the site of past colon surgery in the region of the cecum. Image registration techniques clearly showed ^{131}I-mAbF19 SPECT uptake in the original surgery site in the right iliac fossa (Fig 5). In addition, ^{131}I-mAbF19 SPECT uptake was identified in both the known, right-lobe hepatic metastasis seen by CT, and in the left lobe of the liver adjacent to the stomach, where the CT scan was normal (Fig 4). At surgery, metastatic disease was found at all of these sites.

Biopsy-Based Tumor-to-Liver and Tumor-to-Serum Ratios

Serum samples and biopsies of tumor tissues and adjacent normal liver were obtained for measurement of ^{131}I-mAbF19 uptake and for immunohistochemical detection of FAP (see following). Tumor uptake of ^{131}I-mAbF19 at the time of surgery (7 days post infusion) was found to be as high as 16.5×10^{-3} %ID/g. The tumor-to-serum ratios were up to 9:1 and tumor-to-liver ratios were up to 21:1 at the time of surgery (Fig 6).

Pharmacokinetics

The mean calculated $T_{1/2}$ alpha was 1.12 ± 0.96 hours and the mean calculated $T_{1/2}$ beta was 26.5 ± 17.0 hours. The mean volume of distribution was calculated to be 3.6 ± 1.6 L (Fig 7).

Immunohistochemistry

For 14 of 17 patients included in the study, sufficient biopsy material of metastatic lesions and uninvolved normal liver was available to permit immunohistochemical analyses with acetone-fixed cryostat sections. Parallel

Table 2. Detection of Metastatic Lesions Before and During Surgery

Patient No.	Sites of Disease		
	CT/MRI	^{131}I-mAbF19 SPECT/Planar Images	Surgery
1	Liver: R met	R met (hot) and R met (cold)	R and L met (small)
2	Liver: L met; lung: 0.5-1 cm	L lobe (planar image only)	Liver: L met; lung: met
3	Liver: R met	R and L met	R and L met
4	Liver: R met	R met	R and L (2 cm) met
5	Liver: R met	R and L met, pelvis (RIF)	R and L (2.5 cm) met, pelvic mass
6	Liver: R and L met	R and L met	R and L met; portal LN met
7	Liver: R met	R met	R met (single)
8	Liver: R met	R met	R met
9	Liver: R met	R met	R met
10	Equivocal (CT/MRI)	L met	L met, R met < 1 cm
11	Liver: R and L met	R and L met	R and L met
12	Pelvic mass: equivocal (MRI)	Negative (planar image only)	Pelvic mass
13	Liver: R and L met	R and L met	R and L met, portal LN, visceral seeding
14	Liver: caudate met or periportal LN	Portal LN	Portal LN, liver met < 1 cm
15	Liver: R and L met	R and L met	R and L met, portal LN (1 cm)
16	Liver: equivocal (possible R met 1.5 cm)	Negative (planar image only)	R and L met, ≤ 1.5 cm
17	Liver: R and L met (single)	R and L met (single)	R and L met (single)

NOTE. Length estimates (in centimeters) refer to the diameter of metastatic lesions. In several patients with extensive metastatic disease, no attempt was made during surgery to fully document the number and size of metastatic lesions.

Abbreviations: R, right lobe hepatic lesion, L, left lobe hepatic lesion; met, metastasis/metastases; RIF, right illiac fossa; LN, lymph node metastases.

ReprintsDesk | 3/10/2026 9:56:08 PM

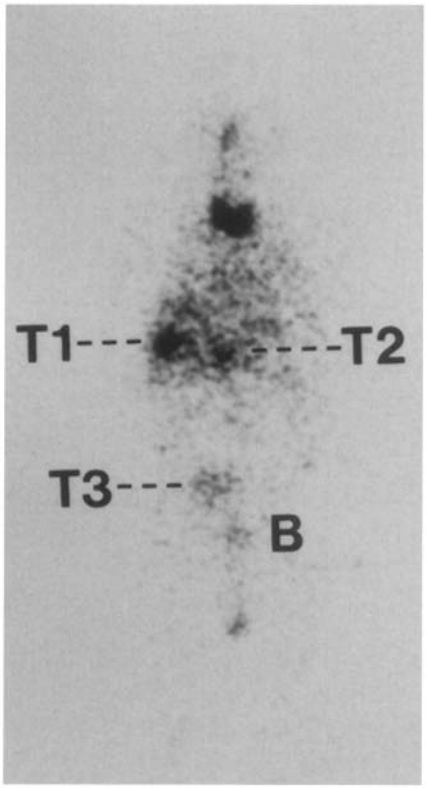

Fig 3. Anterior planar image of patient no. 5 obtained 4 days after infusion of ^{131}I-mAbF19. Patient had a history of increasing serum CEA levels, a solitary right lobe liver lesion seen on CT scan, and equivocal CT changes at the site of past colon surgery in the region of the cecum. A fine-needle biopsy of the right lobe liver lesion had been found to be positive for metastatic colon carcinoma, while a biopsy of the cecal mass was negative for malignant cells. In the planar image, uptake of ^{131}I-mAbF19 is evident in the right lobe liver lesion (T1). In addition, uptake is also seen in the left lobe of the liver (T2), and in the right lower quadrant of the abdomen at the site of past surgery (T3). Bladder activity (B) due to the excretion of free iodine is also evident.

sections were cut and stained with hematoxylin/eosin to confirm the diagnosis, and tested by the avidin-biotin immunoperoxidase method for antigen expression. Three different antigens were routinely tested: FAP, as a marker of reactive stromal fibroblasts; endoGlyx-1 (detected by mAbH572), as a specific marker of vascular endothelial cells; and mAbA33, which identifies an antigen of normal and malignant colonic epithelium. As shown in Fig 8 and listed in Table 1, we found that all hepatic metastases examined contained FAP-positive stromal fibroblasts, whereas samples of uninvolved normal liver lacked detectable FAP expression (Fig 8D). Comparison of the staining patterns for FAP, endoGlyx-1, and A33 allowed us to assess antigen expression with regard to the architecture of the tumor stroma. These experiments showed that the tumor capillaries (endoGlyx-1–positive, Fig 8B) are not generally in immediate contact with the basal aspect of the malignant epithelium (A33-positive, Fig 8C). Instead, the space between the tumor capillaries and between capillaries and epithelial cells is occupied by FAP-positive stromal fibroblasts (Fig 8A) and various extracellular matrix proteins, such as tenascin (not shown), which are expressed diffusely in the extracellular space of the tumor stromal compartment. This characteristic spatial distribution pattern with FAP-positive reactive stromal fibroblasts interposed between tumor capillaries and malignant epithelium was observed in all metastatic lesions examined.

DISCUSSION

The FAP antigenic system combines several attributes that may be critical for developing the stromal targeting concept into new modalities for cancer detection and therapy. These include the highly restricted distribution of FAP in normal tissues, uniform and consistent expression in the stroma of primary and metastatic lesions of common epithelial cancers, and a surface membrane localization.[27,30,31] The present study describes the first step in moving the idea of FAP-directed tumor stromal targeting from the preclinical phase to in vivo evaluation. We report that ^{131}I-mAbF19 shows no toxicity at the dose levels tested and achieves consistent targeting to metastatic lesions in patients with colorectal carcinoma.

This conclusion is based on a study design that incorporates several of the principles established in our previous work[20] with the colorectal carcinoma-reactive mAbA33, as follows: (1) selection of a relatively uniform patient population with liver metastases from colorectal carcinoma; all patients were eligible for resection of localized liver metastases or insertion of hepatic artery catheter for regional chemotherapy. (2) Sequential scanning over 7 to 8 days, using planar imaging, SPECT, and advanced SPECT/CT image registration techniques.[32-34] (3) Biopsy-based dosimetry to establish tumor uptake of ^{131}I-mAbF19 and tumor-to-liver and tumor-to-serum ratios. Finally, (4) immunohistochemical analysis of biopsy specimens to assess levels of FAP expression and to define the spatial arrangement of FAP-positive tumor stromal fibroblasts with regard to tumor capillaries and the malignant colonic epithelial cells.

The peak serum levels and serum $T_{1/2}$ of ^{131}I-mAbF19 are similar to what has been observed for other murine mAbs that do not bind significantly to blood cells or to other accessible normal tissues.[20] Similarly, the induction of HAMA responses in all treated patients was predicted from earlier studies. The optimal time for tumor imaging was 3 to 5 days after ^{131}I-mAbF19 administration. SPECT analysis significantly improved lesion detection when

ReprintsDesk | 3/10/2026 9:56:08 PM

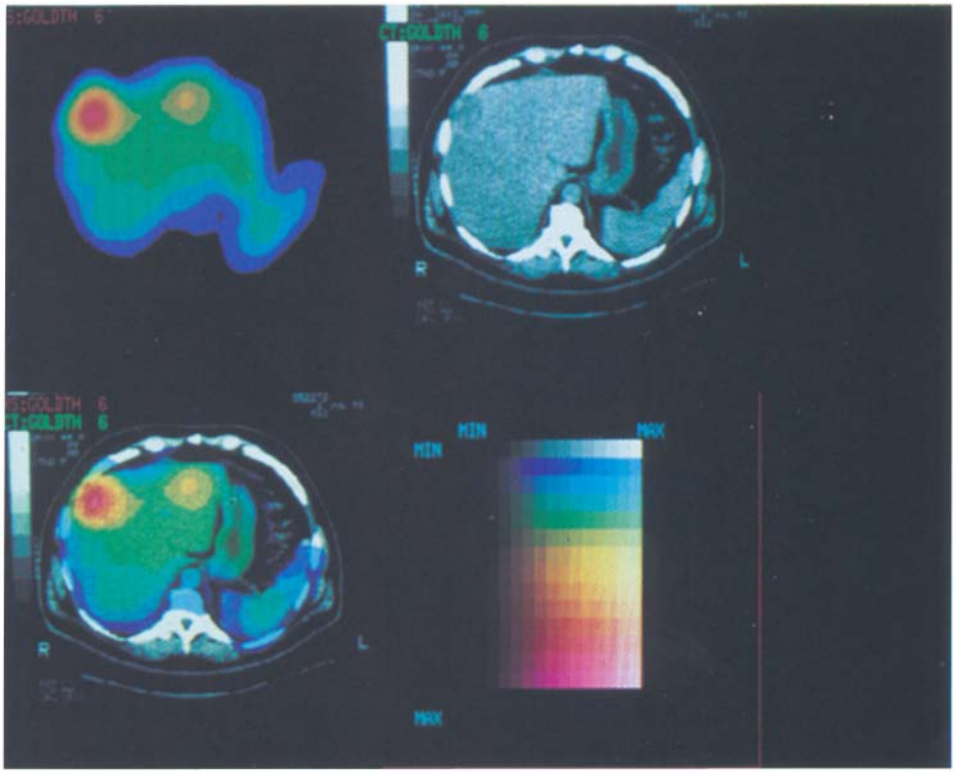

Fig 4. Registered SPECT and CT images of patient no. 5. (Top left) Transverse SPECT section through the liver; (top right) corresponding CT section in the same plane through the liver; (bottom left) SPECT image fused with the CT scan, with the SPECT image displayed in colorwash on the black and white CT image. Uptake of ^{131}I-mAbF19 is seen in the right lobe lesion present on CT scan (T1 in the planar images; see Fig 3). In addition, an area of uptake can be identified in the left lobe anteriorly (T2 in the planar images); the CT scan is normal at this site. At surgery, the right lobe lesion was confirmed as metastatic colon carcinoma, and an additional metastasis (2.5 cm in diameter) was found, located exactly in the area of ^{131}I-mAbF19 SPECT uptake.

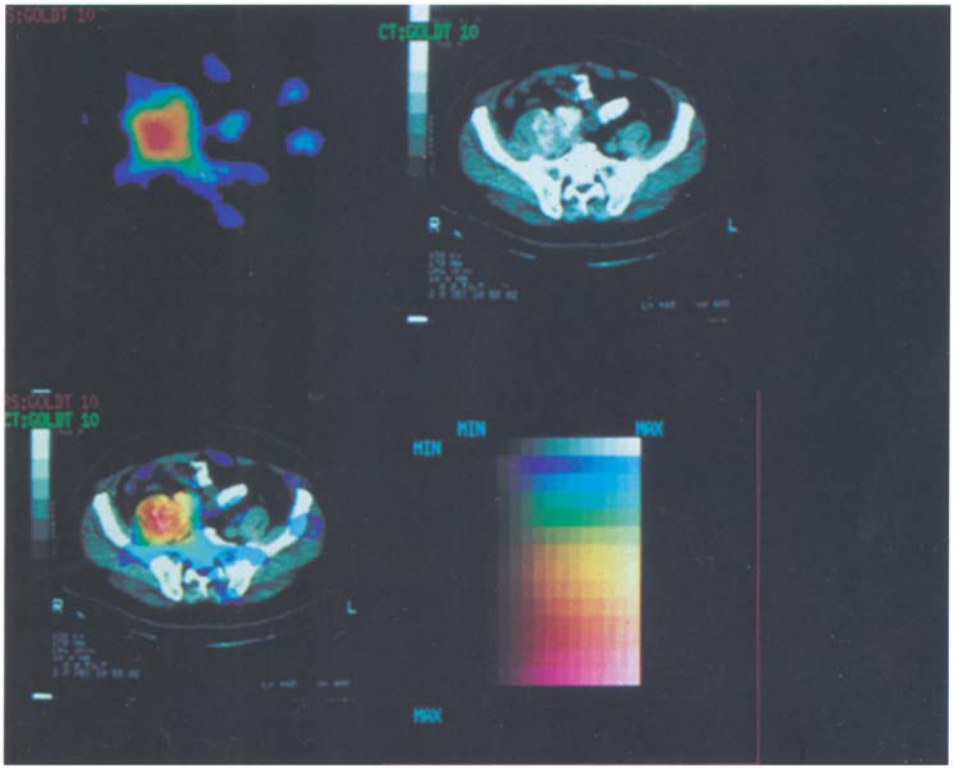

Fig 5. Registered SPECT and CT images of the lower abdomen in patient no. 5. (Top left) Transverse SPECT section through the lower abdomen; (top right) corresponding CT section in the same plane; (bottom left) SPECT image fused with the CT scan, with the SPECT image displayed in colorwash on the CT image. Uptake of ^{131}I-mAbF19 is evident in the residual soft tissue mass at the site of prior surgery. At surgery, this mass was confirmed as recurrent colon carcinoma.

ReprintsDesk | 3/10/2026 9:56:08 PM

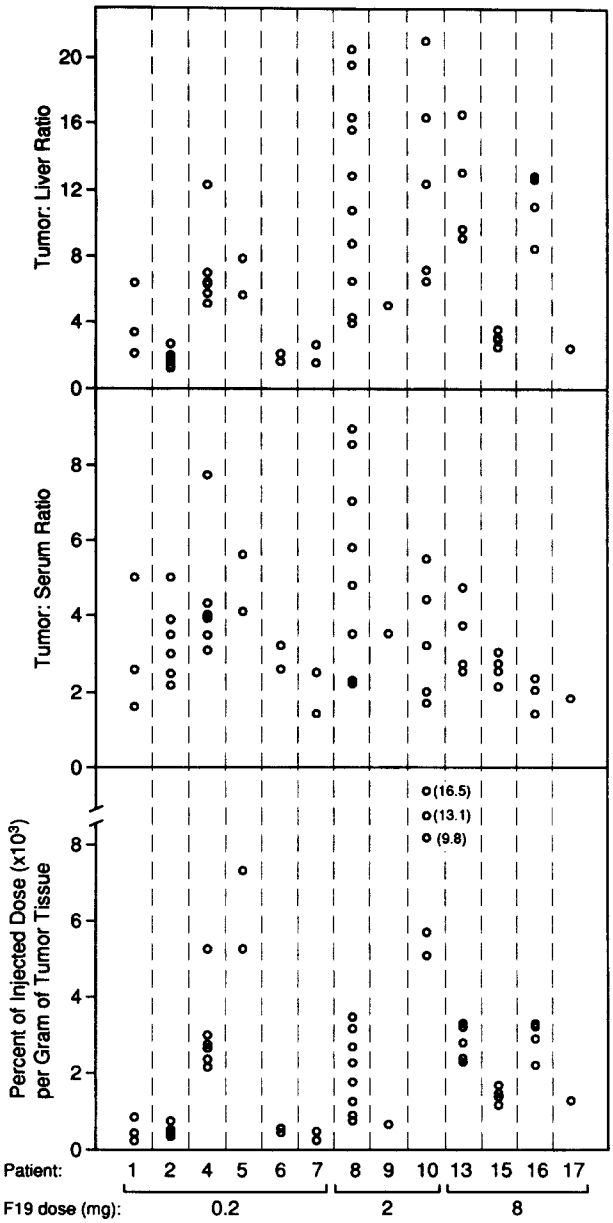

Fig 6. Biodistribution of ^{131}I-mAbF19. Tumor and adjacent normal liver tissues and bloods were obtained from each patient at surgery (7 days after mAb administration).

compared with planar imaging. The smallest lesion visualized was 1 cm in diameter, and lesions more than 2 cm were identified in 15 of 17 patients. In each case, the ^{131}I-mAbF19–positive sites were confirmed as metastatic lesions by biopsy. For the two patients with negative ^{131}I-mAbF19 scans, only planar images were available and it is not known whether SPECT studies would have been positive. In addition to hepatic metastases, extrahepatic lesions in portal lymph nodes and pelvic recurrent disease were also correctly identified on ^{131}I-mAbF19 scans in three patients.

Traditional methods for planar and SPECT imaging with radiolabeled mAbs provide only limited information about the anatomic sites of mAb uptake. Yet, the ability to map these sites to precise anatomic structures is of considerable interest for the development of imaging and immunotherapy methods. A significant advance in lesion mapping has come from recently developed SPECT and CT/MRI image registration techniques.[32-34] In the present study, the added resolution provided by these image registration techniques was clearly demonstrable for ^{131}I-mAbF19 SPECT analyses.

The present study was designed primarily to study the toxicity of ^{131}I-mAbF19 and to provide proof-of-principle for the concept of stromal targeting in patients with solid neoplasms. It is too limited in scope to allow any firm conclusions to be drawn about the sensitivity of lesion detection with ^{131}I-mAbF19 SPECT and for comparisons with other radiologic methods. Nevertheless, our findings for individual patients suggest that ^{131}I-mAbF19 scans may complement the information obtained from CT/MRI scans in some patients. For example, in patient no. 5, ^{131}I-mAbF19 SPECT identified three distinct lesions, namely, two hepatic metastases and a pelvic mass. By contrast, CT showed only one of the two hepatic metastases, and the pelvic mass was interpreted as probable scarring at the site of primary surgery. Biopsies showed that all three sites identified by ^{131}I-mAbF19 SPECT contained tumor.

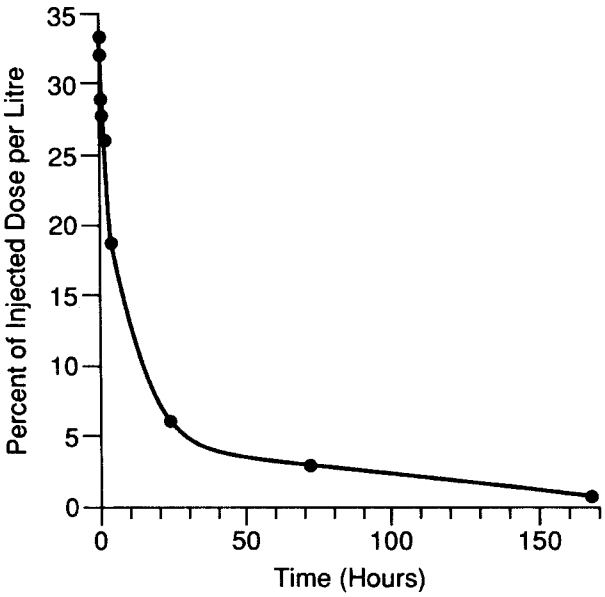

Fig 7. Representative mean serum clearance curve of ^{131}I-mAbF19. The rapid early clearance and mean $T_{1/2}$ of 26.5 hours is similar to that of other murine mAbs.

ReprintsDesk | 3/10/2026 9:56:08 PM

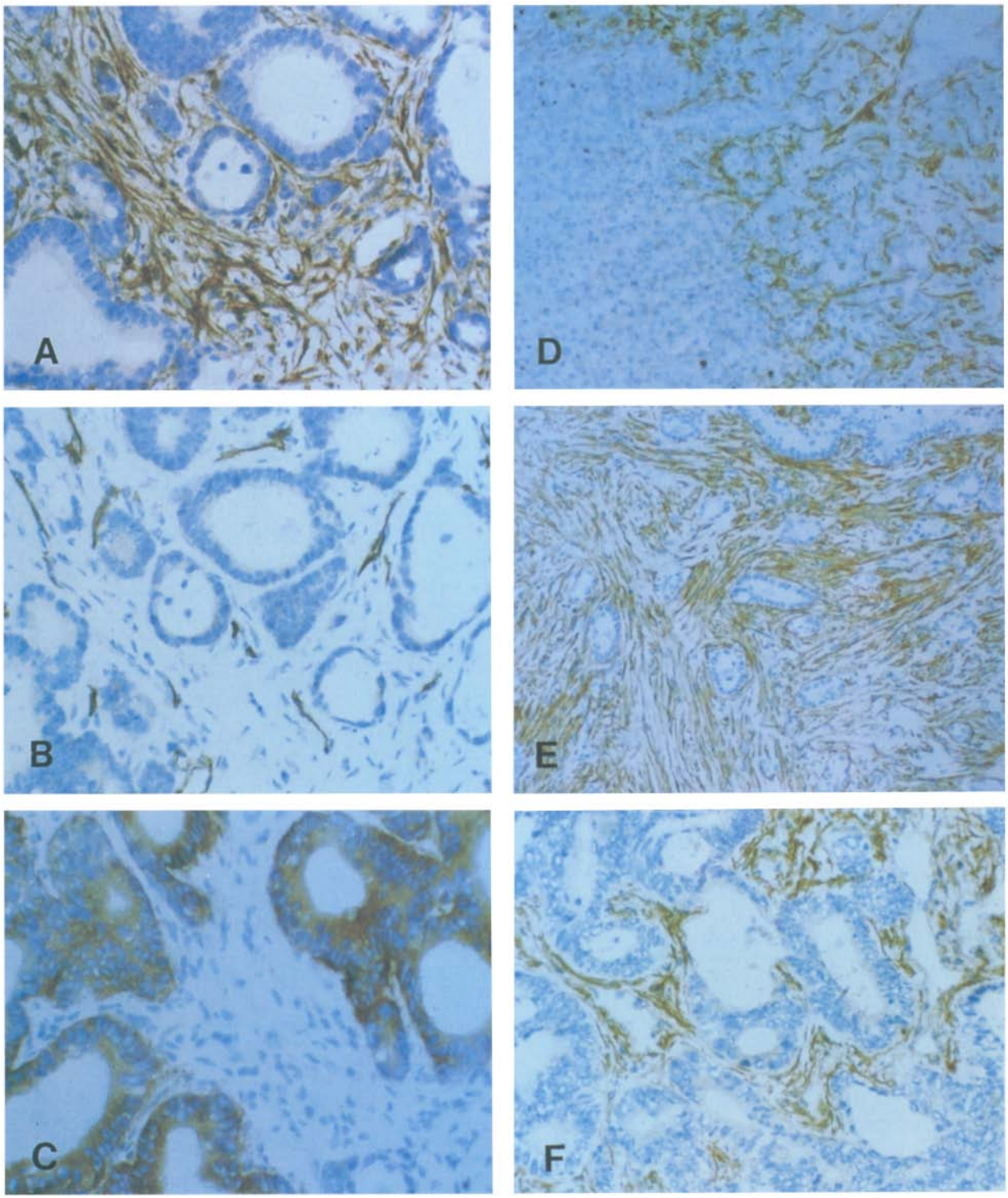

Fig 8. Immunohistochemical analysis of metastatic colorectal carcinomas. Serial sections of a hepatic metastasis from patient no. 6 (A to C) were stained with mAbF19 to identify FAP-positive reactive stromal fibroblasts (A), mAbH572 to label tumor capillaries (B), and mAbA33 to identify epithelial tumor cells (C). (D) Hepatic metastasis from patient no. 16 stained with mAbF19; note the presence of FAP-positive stromal fibroblasts in the metastatic lesion (right), but not in the adjacent uninvolved liver (left). (E) Hepatic metastasis from patient no. 4 stained with mAbF19; note abundant stromal compartment interspersed with malignant epithelial cell clusters. (F) Metastatic lesion from patient no. 1 stained with mAbF19 shows a scanty, FAP-positive stromal compartment. Cryostat sections of frozen tissues were acetone-fixed and stained by the avidin-biotin immunoperoxidase procedure, followed by counterstaining with Harris' hematoxylin. Negative control experiments with irrelevant mouse IgG1 were included in all assays and did not produce any staining.

ReprintsDesk | 3/10/2026 9:56:08 PM

Accumulation of ^{131}I-mAbF19 in metastatic lesions was also demonstrated by biopsy-based dosimetry studies. The sequential imaging studies suggested that optimal tumor-to-normal tissue ratios were achieved 3 to 5 days after mAb administration, but because of the initial design of the study protocol, surgery and biopsies were not performed until day 7 in the present study. At the time of surgery, ^{131}I-mAbF19 uptakes in the metastatic tumor tissues ranged from 0.001 to 0.016%ID/g.

An important consideration in developing the concept of tumor stromal targeting in solid neoplasms is the precise architecture of the stromal compartment, which may determine the accessibility of stromal antigens to circulating mAbs and the choice of optimal effector functions for stroma-specific mAbs. In agreement with previous immunohistochemical findings, we found that all of the hepatic metastases examined contained significant numbers of FAP-positive reactive stromal fibroblasts, whereas malignant epithelial cells and uninvolved normal liver were FAP-negative.[27,30,31] The amount of stroma present in individual biopsy samples varied considerably. Although multiple sites of the biopsy samples were tested for each patient, it is not yet clear whether the observed differences in the amount of stroma reflect intrinsic differences between tumors in individual patients or incomplete sampling of larger tumor masses. A clearer picture emerged with regard to the spatial arrangement of FAP-positive fibroblastic cells within metastatic lesions. In each case tested, the FAP-positive cells were arranged around tumor capillaries, often occupying the narrow spaces that separate the tumor blood vessels from the basal aspect of the malignant epithelium. This strategic location may be critical to insure accessibility of FAP antigens to circulating mAb and for the design of specific effector functions.

One concern in the development of stromal targeting for cancer therapy is based on the notion that the stromal response to cancer and in wound healing may be similar at the cellular and molecular level,[22-25] and FAP is known to be expressed transiently in healing dermal incision wounds.[31] Despite the fact that the patients included in the present study had undergone prior surgery and consequently had extensive abdominal scars, we did not observe any ^{131}I-mAbF19 localization to these sites. FAP expression in wound healing may well be too transient to be detectable several months or years after surgery. Alternatively, some FAP-positive stromal fibroblasts may persist in aged wounds but, due to the limited blood supply to scar tissue, may be less accessible to circulating mAbF19 than tumor stromal fibroblasts.

The murine ^{131}I-mAbF19 used in the present study has no known tumoricidal activity and was not expected to show significant therapeutic effects. However, having demonstrated that the murine mAbF19 can target tumor sites effectively, it is now possible to develop recombinant forms of mAbF19, or mAbF19 conjugates with improved pharmacokinetic properties, low immunogenicity to permit retreatment, and novel antitumor effector functions. Of particular interest will be the derivation of humanized forms of mAbF19, the construction of mAbF19 conjugates with radioisotopes or radiometal chelates that permit bystander killing of tumor cells, or the production of mAbF19 versions with potent inflammatogenic properties, which may focus host immune responses on tumor sites. Finally, the stromal compartment may not only be important for nutrient and oxygen supply of tumor cells, but also as a source of growth factors and proteolytic enzymes.[36,37] Consequently, mAbs that inhibit stromal cell function may inhibit tumor growth, and studies aimed at defining the role of FAP in the growth and invasiveness of solid neoplasms are in progress.

ACKNOWLEDGMENT

We thank M. John for help with the production, purification, and quality control of mAbF19.

REFERENCES

1. Goldenberg D: Future role of monoclonal antibodies in oncologic diagnosis and therapy. Semin Nucl Med 19:332-339, 1989

2. Mach JP, Pelegrin A, Buchegger F: Imaging and therapy with monoclonal antibodies in non-hematopoietic tumors. Curr Opin Immunol 3:685-693, 1991

3. Larson SM: Lymphoma, melanoma, colon cancer: Diagnosis and treatment with radiolabeled monoclonal antibodies. Radiology 165:298-304, 1987

4. Sands H: Experimental studies of radioimmunodetection of cancer: An overview. Cancer Res 50:809-813, 1990 (suppl)

5. Jain RK: Delivery of novel therapeutic agents in tumors: Physiological barriers and strategies. J Natl Cancer Inst 81:570-576, 1989

6. Waldmann TA: Monoclonal antibodies in diagnosis and therapy. Science 252:1657-1662, 1991

7. Press OW, Eary JF, Applebaum FR, et al: Radiolabeled-antibody therapy of B-cell lymphoma with autologous bone marrow support. N Engl J Med 329:1219-1224, 1993

8. Trail PA, Willner D, Lasch SJ, et al: Cure of xenografted human carcinomas by BR96-doxorubicin immunoconjugates. Science 261:212-215, 1993

9. Levy R, Miller RA: Therapy of lymphoma directed at idiotypes. J Natl Cancer Inst Monogr 10:61-68, 1990

10. Riethmüller G, Johnson JP: Monoclonal antibodies in the detection and therapy of micrometastatic epithelial cancers. Curr Opin Immunol 4:647-655, 1992

11. Rettig WJ: Immunogenetics of cell surface antigens of human cancer. Curr Opin Immunol 4:630-640, 1992

12. Winter G, Milstein C: Man-made antibodies. Nature 349:293-299, 1991

ReprintsDesk | 3/10/2026 9:56:08 PM

13. Pastan I, Fitzgerald D: Recombinant toxins for cancer treatment. Science 254:1173-1177, 1991

14. Hinman LM, Hamann PR, Wallace R, et al: Preparation and characterization of monoclonal antibody conjugates of the calicheamicins: A novel and potent family of antitumor antibiotics. Cancer Res 53:3336-3344, 1993

15. Caron PC, Class K, Laird W, et al: Enhanced biological and immunological properties of CDR-grafted multimeric human immunoglobulins. J Exp Med 176:1191-1195, 1992

16. Reisfeld RA, Mueller BM, Schrappe M, et al: Antibody-drug conjugates for cancer therapy: promises and problems. Immunol Allergy Clin North Am 11:341-358, 1991

17. Gillies SD, Young D, Lo KM, et al: Expression of genetically engineered immunoconjugates of lymphotoxin and a chimeric anti-ganglioside GD2 antibody. Hybridoma 10:347-356, 1991

18. Gansow OA, Brechbiel MN, Mirzadeh S, et al: Chelates and antibodies: Current methods and new directions. Cancer Treat Res 51:153-171, 1992

19. Bird RE, Hardmann KD, Jacobson JW, et al: Single-chain antigen-binding proteins. Science 242:423-426, 1988

20. Welt S, Divgi CR, Real FX, et al: Quantitative analysis of antibody localization in human metastatic colon cancer: A phase I study of monoclonal antibody A33. J Clin Oncol 8:1894-1906, 1990

21. Oosterwijk E, Bander NH, Divgi CR, et al: Antibody localization in human renal cell carcinoma: A phase I study of monoclonal antibody G250. J Clin Oncol 11:738-750, 1993

22. Folkman J: Tumor angiogenesis. Adv Cancer Res 43:175-203, 1984

23. Denekamp J: Vascular attack as a therapeutic strategy for cancer. Cancer Metastasis Rev 9:267-282, 1990

24. van den Hoff A: The role of stromal cells in tumor metastasis: A new link. Cancer Cells 3:186-187, 1991

25. Dvorak HF, Nagy JA, Dvorak AM: Structure of solid tumors and their vasculature: Implications for therapy with monoclonal antibodies. Cancer Cells 3:77-85, 1991

26. Rettig WJ, Garin-Chesa P, Healey JH, et al: Identification of endosialin, a cell surface glycoprotein of vascular endothelial cells in human cancer. Proc Natl Acad Sci USA 89:10832-10836, 1992

27. Garin-Chesa P, Old LJ, Rettig WJ: Cell surface glycoprotein of reactive stromal fibroblasts as a potential antibody-target in human epithelial cancers. Proc Natl Acad Sci USA 87:7235-7239, 1990

28. Burrows AJ, Watanabe Y, Thorpe PE: A murine model for antibody-directed targeting of vacular endothelial cells in solid tumors. Cancer Res 52:5954-5962, 1992

29. Rettig WJ, Garin-Chesa P, Beresford HR, et al: Differential expression of cell surface antigens and glial fibrillary acidic protein in human astrocytoma subsets. Cancer Res 46:6406-6412, 1986

30. Rettig WJ, Garin-Chesa P, Healey JH, et al: Regulation and heteromeric structure of the fibroblast activation protein in normal and transformed cells of mesenchymal and neuroectodermal origin. Cancer Res 53:3327-3335, 1993

31. Rettig WJ, Garin-Chesa P, Beresford HR, et al: Cell surface glycoproteins of human sarcomas: Differential expression in normal and malignant tissues and cultured cells. Proc Natl Acad Sci USA 85:3110-3114, 1988

32. Scott AM, Macapinlac H, Divgi CR, et al: Clinical validation of SPECT and CT/MRI registration in radiolabeled monoclonal antibody studies of colorectal carcinoma. J Nucl Med 34:94P, 1993 (abstr)

33. Scott AM, Macapinlac H, Zhang J, et al: Clinical applications of fusion imaging in oncology. Nucl Med Biol (in press)

34. Pelizzari CA, Chen GTY, Spelbring DR, et al: Accurate three-dimensional registration of CT, PET and/or MRI images of the brain. J Comput Assist Tomogr 14:20-26, 1989

35. Rettig WJ, Erickson HP, Albino AP, Garin-Chesa P. Induction of human tenascin (neuronectin) by growth factors and cytokines: cell type-specific signals and signalling pathways. J Cell Sci 107:487-497, 1994

36. Basset P, Belloq JP, Wolf C, et al: A novel metalloproteinase gene specifically expressed in stromal cells of breast carcinomas. Nature 348:699-704, 1990

37. Cullen KJ, Smith HS, Hill S, et al: Growth factor messenger RNA expression by human breast fibroblasts from benign and malignant lesions. Cancer Res 51:4978-4985, 1991